

1321

1322 *Paleoceanography and Paleoclimatology*

1323 Supporting Information for

1324 **Drastic Vegetation Change in the La Guajira Peninsula (Colombia) during the Neogene**1325 Carlos Jaramillo<sup>1,2,3</sup>, Pierre Sepulchre<sup>4</sup>, Damian Cardenas<sup>1,5</sup>, Alexander Correa-Metrio<sup>6</sup>, J. Enrique  
1326 Moreno<sup>1</sup>, Raul Trejos<sup>7</sup>, Diego Vallejos<sup>7</sup>, Natalia Hoyos<sup>8</sup>, Camila Martínez<sup>1</sup>, Daniella Carvalho<sup>1</sup>,  
1327 Jaime Escobar<sup>8,1</sup>, Francisca Oboh-Ikuenobe<sup>5</sup>, Mercedes B. Prámparo<sup>9</sup>, and Diego Pinzón<sup>9</sup>1328 <sup>1</sup>Smithsonian Tropical Research Institute, Panamá.1329 <sup>2</sup>ISEM, U. Montpellier, CNRS, EPHE, IRD, Montpellier, France.1330 <sup>3</sup>Department of Geology, Faculty of Sciences, University of Salamanca, Salamanca 37008, Spain.1331 <sup>4</sup>Laboratoire des Sciences du Climat et de l'Environnement, LSCE/IPSL, CEA-CNRS-UVSQ, Université Paris-Saclay, F-  
1332 91191 Gif-sur-Yvette, France.1333 <sup>5</sup>Department of Geosciences and Geological and Petroleum Engineering, Missouri University of Science and  
1334 Technology, Rolla, MO, USA.1335 <sup>6</sup>Instituto de Geología, Universidad Nacional Autónoma de México, Mexico.1336 <sup>7</sup>Department of Geology, Universidad de Caldas, Manizales, Colombia.1337 <sup>8</sup>Universidad del Norte, Barranquilla, Colombia.1338 <sup>9</sup>IANIGLA, CCT-CONICET, Mendoza, Argentina.

1339

1340

1341

1342 **Contents of this file**

1343

1344 **Section S1 Detailed biostratigraphic analysis**1345 **Figure S1.** Chorographic chart of the Maracaibo Lake, "Carta corográfica de la Laguna de  
1346 Maracaibo" (Archivo\_General\_da\_las\_Indias, 1744).1347 **Figure S2.** Modern Ecosystem Map of Cocinetas basin. Independent variables used to predict  
1348 ecosystem class within a random forest classification: (a) elevation, (b) slope, (c) distance to  
1349 coastline, (d) distance to streams, (e) geologic units, (f) land cover, (g) red-band reflectance, (h)  
1350 shortwave-infrared-band reflectance, (i) NDVI.1351 **Figure S3.** Map of the Guajira Peninsula with the geographic location of meteorological  
1352 stations. Stations in blue record monthly precipitation with average annual precipitation in

1353 parenthesis. Stations in red record monthly temperature. Map color scale represents terrain  
1354 elevation in meters above sea level (masl).

1355 **Figure S4.** Training dataset for the climatic model. We used 1,142,524 occurrences but the  
1356 environmental distribution is unequal with fewer datapoints in the dry end of the precipitation  
1357 spectrum that could produce a bias in the climatic .

1358 **Figure S5.** Landsat images during (a) El Niño and (b) La Niña events.

1359 **Table S1.** Historical Accounts of vegetation in the Guajira Peninsula.

1360 **Table S2.** Data sources for modern ecosystems map.

1361 **Table S3.** Location of Holocene samples

1362

1363 **Additional Supporting Information (Files uploaded separately in Zenodo,**  
1364 **DOI:10.5281/zenodo.4075108)**

1365 **Data Set S1.** Counts of foraminifera, nannoplankton and palynomorphs of samples in Well A  
1366 and Holocene samples

1367 **Data Set S2.** Palynological Plates of the taxa found in Well A

1368 **Model Outputs.** Figures 9 and 10 were done using NOAA pyferret within Jupyter notebooks,  
1369 thanks to the ferretmagic add-on developed at LSCE by Patrick Brockmann. Ferret is a product  
1370 of NOAA's Pacific Marine Environmental Laboratory.(Information is available at  
1371 <http://ferret.pmel.noaa.gov/Ferret> (lastaccess: 1 June 2020; NOAA's Pacific Marine  
1372 Environmental Laboratory, 2020)), distributed under the Open Source Definition. The Jupyter  
1373 notebook is an open-source web application. Figures 9 and 10 in this paper were made with  
1374 perceptually uniform, color-vision-deficiency-friendly scientific color maps, developed and  
1375 distributed by Fabio Crameri (<http://www.fabiocrameri.ch/colourmaps.php>), to prevent visual  
1376 distortion of the data (Crameri et al., 2018)

1377

1378 **Section S1. Detailed biostratigraphic analysis**

1379 There are extensive studies using outcrops in the Cocinetas Basin, mostly focused  
1380 on the Castilletes and Jimol Formations (Jaramillo et al., 2015; Moreno et al., 2015).  
1381 These studies have provided a solid time control based upon molluscan Sr stratigraphy  
1382 (Hendy et al., 2015). Based upon the age model for the Jimol and Castilletes formations  
1383 proposed by Hendy et al. (2015) ( $y = -0.0058x + 16.722$ , y is time in Ma, x is the  
1384 stratigraphic meter using zero as the Castilletes/Jimol contact, see Hendy et al. (2015) for  
1385 further details), the uppermost part of the WA (39.6 m) would be ~17.3 Ma (Figure 2)  
1386 and the Uitpa-Jimol contact, that is at 393.2 m (1290') would be 19.4 Ma (Figure 2). The  
1387 presence of the calcareous nannofossil *Helicosphaera ampliaperta* (20.43-14.86 Ma)  
1388 (Backman et al., 2012) at the top of WA also supports a Burdigalian age for the upper  
1389 segment.

1390                  The LAD of the planktonic foraminifera *Ciperoella ciperoensis* is at 752.9 m  
1391 (2470') dated as 22.9 Ma (Olsson et al., 2018; Wade et al., 2011), at the base of the  
1392 Miocene, while the LAD of the spore *Cicatricosisporites dorogensis* is at 762 m (2500'),  
1393 which defines the top of palynological zone T-11 (Jaramillo et al., 2011) dated as the  
1394 Oligocene/Miocene boundary (Jaramillo et al., 2011). The WA has a single occurrence of  
1395 *Paragloborotalia cf. P. kugleri* at 734.6 m (2410'), and the first appearance datum (FAD)  
1396 of this taxon is considered an indicator of the base of the M1 zone (Oligocene/Miocene  
1397 boundary) (Hilgen et al., 2012; Leckie et al., 2018; Wade et al., 2011). However, we  
1398 prefer to use LAD events when dealing with ditch-cutting samples to avoid biases due to  
1399 caving.

1400                  The position of the Miocene-Oligocene boundary is also supported by both  
1401 planktonic foraminifera and calcareous nannofossils. The co-occurrence in the interval  
1402 734.6-871.7 m (2410'-2860') of planktonic foraminifera *Dentoglobigerina galavisi*,  
1403 *Dentoglobigerina globularis*, *Dentoglobigerina larmeui*, and *Globigerinella*  
1404 *praesiphonifera* indicates an earliest Miocene to early Oligocene age between planktonic  
1405 foraminifera biozones O4 – M1b of Wade et al. (2011) (taxa biozones after (Spezzaferri  
1406 et al., 2018; Wade et al., 2018)). *Helicosphaera compacta* occurs at 835.2-844.3 m  
1407 (2740'-2770') and this taxon ranges into the nannoplankton biozone NP24 of Martini that  
1408 has been dated as late Oligocene (Chattian) (Agnini et al., 2014; Martini, 1971; Perch-  
1409 Nielsen, 1985). An Oligocene age for the lowermost Uitpa Formation is also supported  
1410 by the occurrences of *Cyclicargoliyhus abisectus* 688.9-871.7 m (2260'-2860') and  
1411 *Sphenolithus umbrellus* at 752.9-798.6 m (2470'-2620') whose appearances have been  
1412 reported for the early and late Oligocene, respectively (Aubry, 2014; Varol, 1998). The  
1413 LAD of both *C. abisectus* and *Reticulofenestra bisecta* at 688.9 m (2260') (Figure 2)  
1414 together with the sporadic occurrence of *Helicosphaera recta* at 734.6-880.9 m (2410'-  
1415 2890') (Data Set S1) constrains the age of the 725.4-826 m (2380'-2710') interval to the  
1416 late Oligocene (Chattian) and the earliest Miocene (Aquitianian) (Young, 1998). There  
1417 are occurrences of *Sphenolithus belemnos* from 438.9 m (1440') to 734.6 m (2410'). *S.*  
1418 *belemnos* ranges from 19.01 Ma to 17.96 Ma (Backman et al., 2012) and it is found with  
1419 older assemblages in WA, therefore, we interpret the occurrences to be due to caving.

1420                  Assuming a constant sedimentation rate within the middle/upper Uitpa and using  
1421 the top of the Oligocene at 762 m (2500') and 19.4 Ma at 393.2 m (1290'), the  
1422 Aquitanian/Burdigalian boundary would be at ~495.6 m (1626'). The age of the lower  
1423 part of the Uitpa Formation has been controversial. While an Oligocene to early Miocene  
1424 age was proposed by Becker and Dusenbury (1958) based on benthic foraminifera,  
1425 Lockwood (1965) and Rollins (1965) suggested an early Miocene age (Aquitianian) based  
1426 on foraminifera and ostracods. Becker and Dusenbury (1958) described 137 species of  
1427 foraminifera in six samples of the Uitpa Formation. However, the stratigraphic position  
1428 of each sample within the Uitpa Formation is unknown. Lockwood (1965) is a PhD  
1429 dissertation that mapped extensive areas of the Guajira Peninsula for the first time. He  
1430 collected samples near the base, that were identified by Hermann Duque to belong to the  
1431 *Globorotalia kugleri* zone while samples from the lower middle portion correspond to the  
1432 zone of *Catapsydrax dissimilis* (cited as pers.comm. of Herman Duque, 1965, p. 152-153  
1433 in Lockwood 1965).

1434 Rollins (1965, p. 53) reports that A. B. Whitman recognized three planktonic  
1435 foraminifera zones in the Uitpa, from top to base, *Catapsydrax stainforthi*, *Catapsydrax*  
1436 *dissimilis* and *Globorotalia kugleri*. However, neither Lockwood nor Rollins report a list  
1437 of planktonic foraminifera taxa, making difficult to evaluate this information. The  
1438 *Globorotalia kugleri* zone was considered as late Oligocene by Bolli and Saunders (1985)  
1439 emending the Bolli 1957 zone.

1440 The LADs of the dinocysts *Achomosphaera alcicornu* (27.0 Ma) and  
1441 *Chiropertidium galea* (23.98 Ma) in equatorial latitudes has been proposed to be  
1442 restricted to the Oligocene (Williams et al., 2004). *C. galea* LAD at 856.5 m (2810')  
1443 (~23.9 Ma, Figure 2). The LAD of *A. alcicornu* is at 487.7 m (1600'), extending its range  
1444 in the southern Caribbean to the earliest Burdigalian (~20.3 Ma) (Figure 2). A recent  
1445 study in Panama also supports a younger *A. alcicornu* LAD for the tropical Americas  
1446 (Perez-Consuegra et al., 2018a). Similarly, the range of *Cleistosphaeridium*  
1447 *diversispinosum* has been restricted to the Ypresian–Rupelian in temperate latitudes  
1448 (Eaton et al., 2001; Köthe & Piesker, 2007), but it was consistently recorded throughout  
1449 the entire WA sequence (Data Set S1). Therefore, the LAD of *C. diversispinosum*  
1450 extends at least to the late Burdigalian (~17.3 Ma) in the Southern Caribbean. *C.*  
1451 *diversispinosum* has also been recorded in Aquitanian–Langhian deposits from Egypt  
1452 (Soliman et al., 2012), supporting a younger LAD in lower latitudes.

1453 The LAD of *Cribroperidinium tenuitabulatum* occurs at 85.3 m (280') (~17.6 Ma,  
1454 Figure 2). The LAD of this taxon also occurs in the mid-Burdigalian (~17.4 Ma) in the  
1455 central Llanos of Colombia (Jaramillo et al., 2011). The FAD of *Trinovantedinium*  
1456 *ferugnomatum* at 204.2 m (670') (~18.3 Ma, Figure 2) is younger than its ~16.5 Ma FAD  
1457 for temperate latitudes (Louwye et al., 2008).

1458 The peridiniacean dinocyst *Cristadinium* sp. of De Verteuil & Norris 1992 (De  
1459 Verteuil & Norris, 1992) (Figure 4E) and the acritarch *Quadrina* “incerta” of Jaramillo et  
1460 al. 2017 (2017) (Figure 4O) represent two informal taxa with potentially useful  
1461 stratigraphic ranges. Although *Cristadinium* sp. of De Verteuil & Norris 1992 has been  
1462 reported in Serravallian deposits in the US east coast (De Verteuil and Norris, 1992, as  
1463 undescribed protoperidiniacean species that may be attributable to *Cristadinium*,  
1464 (Edwards et al., 2018)), its continuous record in WA spans the late Chattian–Aquitian  
1465 interval (Data Set S1). The LAD of *Cristadinium* sp. of De Verteuil & Norris 1992  
1466 occurs at 533.4 m (1750') (~20.8 Ma, Figure 2). The single occurrence at 85.3 m (280')  
1467 (~17.6 Ma, Figure 2) of *Quadrina* “incerta” of Jaramillo et al. 2017 is consistent with its  
1468 reports in late Burdigalian deposits in the Gulf of Mexico ((Lenoir & Hart, 1986) as  
1469 Dinocyst XI) and extends its previous LAD (mid-Burdigalian, 18.03 Ma) for  
1470 northwestern South America (Jaramillo et al., 2017).

1471 The LAD of *Quadrina?* *condita* at 615.7 m (2020') (~21.6 Ma, Figure 2) differs  
1472 from previous stratigraphic records suggesting a mid-Burdigalian–Messinian range  
1473 ((Duffield & Stein, 1986) as *Incertae sedis* sp. A; De Verteuil and Norris, 1992). Recent  
1474 analyses indicate a FAD for *Q.?* *condita* at ~18.2 Ma during the onset of a Miocene  
1475 marine incursion event in northwestern South America (Jaramillo et al., 2017). Our  
1476 results indicate an older FAD (not younger than mid-Aquitian) for *Q.?* *condita* in the  
1477 Southern Caribbean. Neogene dinocyst biostratigraphic events for the Southern  
1478 Caribbean differ from those in temperate latitudes, as it has been previously indicated

1479 by Oligocene–Miocene dinocyst assemblages from eastern Venezuela (Helenes &  
 1480 Cabrera, 2003). Therefore, further detailed palynological analyses of equatorial sections  
 1481 are needed to constrain the stratigraphic ranges of marine palynomorphs in low latitudes.

Overall, the biostratigraphic analysis indicates that the WA section spans from the latest Oligocene to early Miocene (late Chattian to Burdigalian) (Figure 2). The top of the Siamana Formation is late Chattian (late Oligocene) while the Uitpa Formation spans from the latest Oligocene to the early Burdigalian (~19.4 Ma). Well A started drilling in the lower part of the Jimol Formation at a stratigraphic level dated as Burdigalian (~ 17.3 Ma).

1488  
1489  
1490

1491

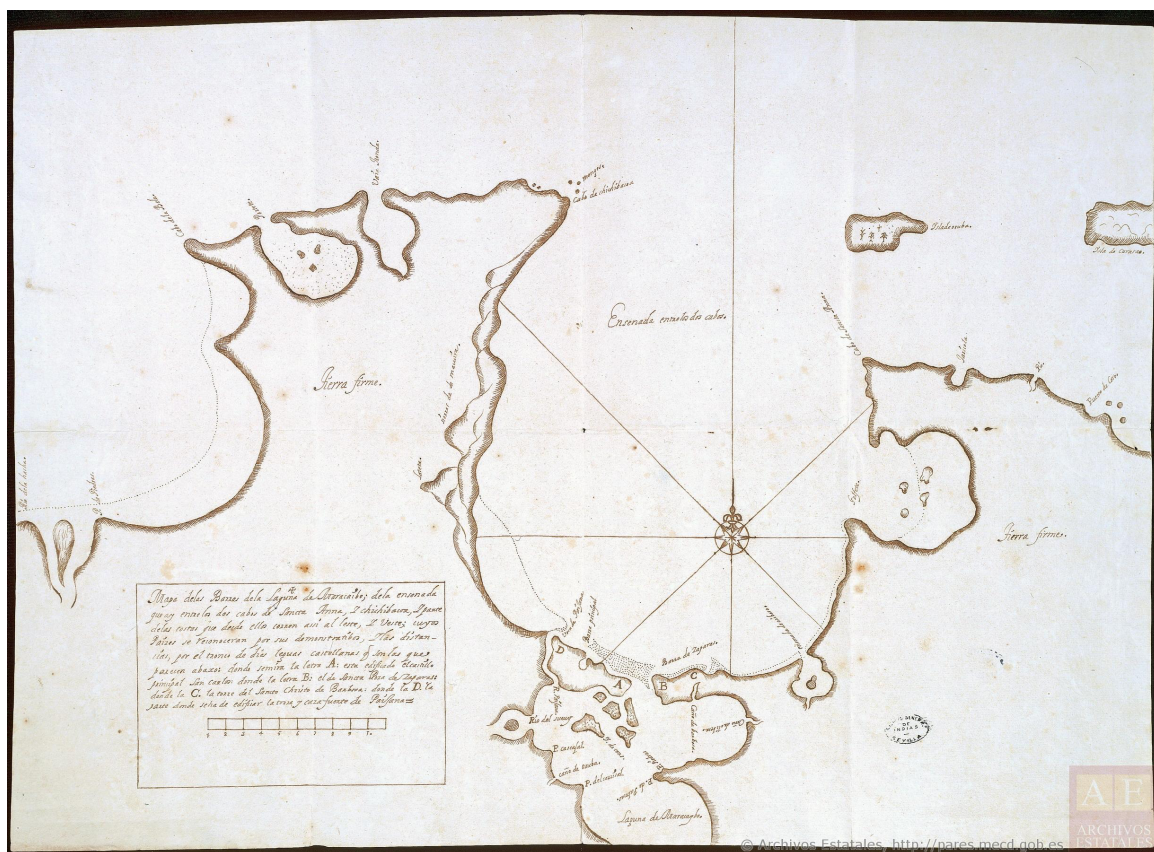
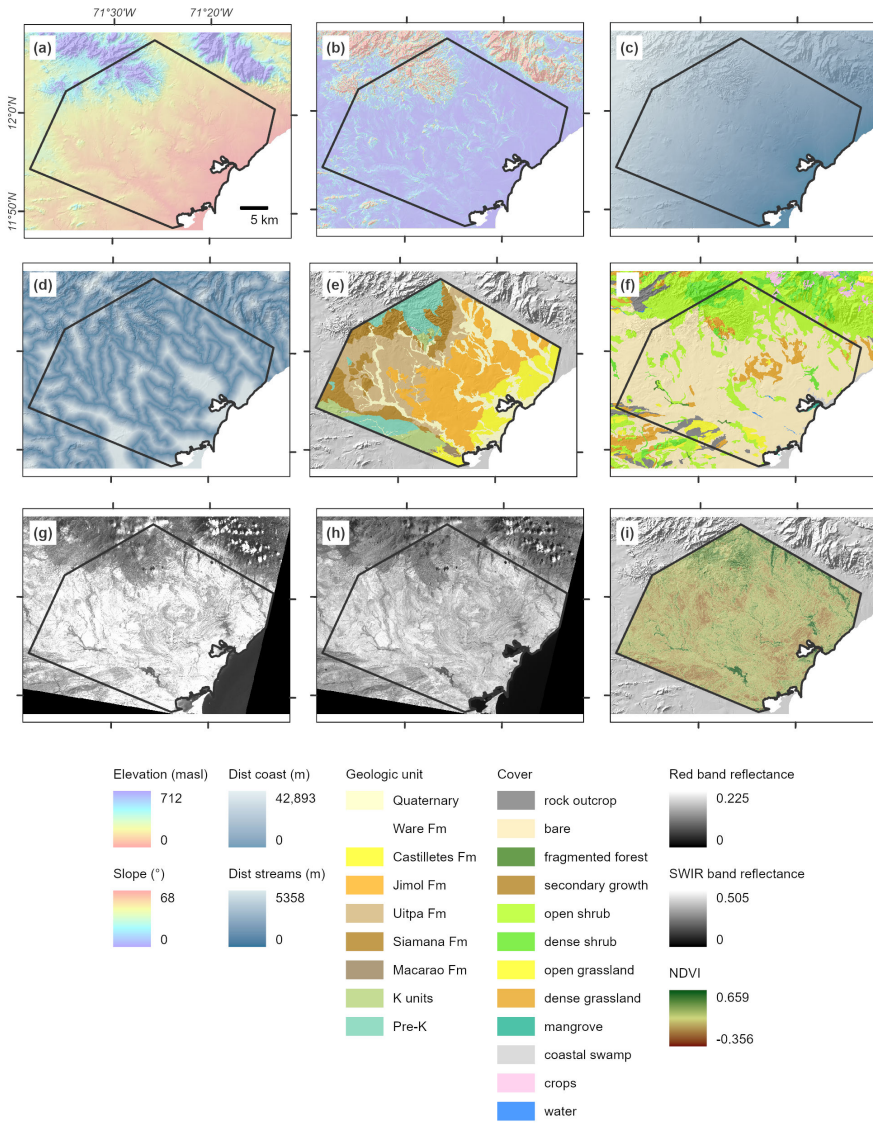
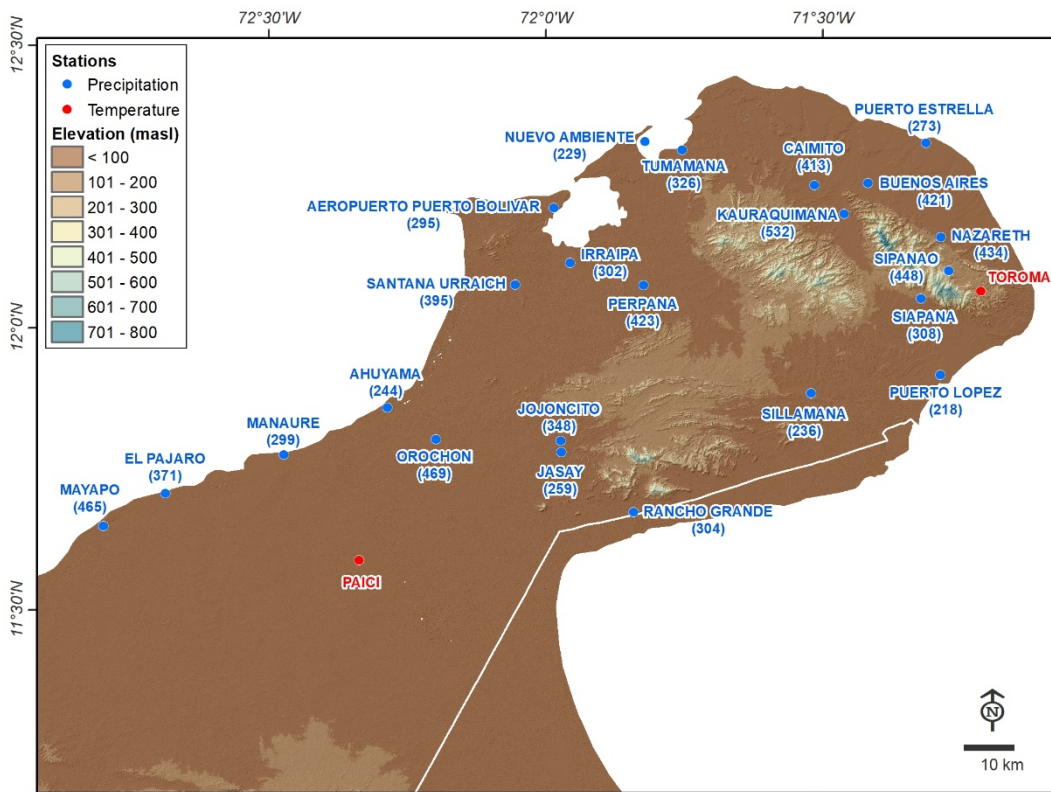


**Figure S1.** Chorographic chart of the Maracaibo Lake, "Carta corográfica de la Laguna de Maracaibo" (Archivo General da las Indias. 1744).



1495

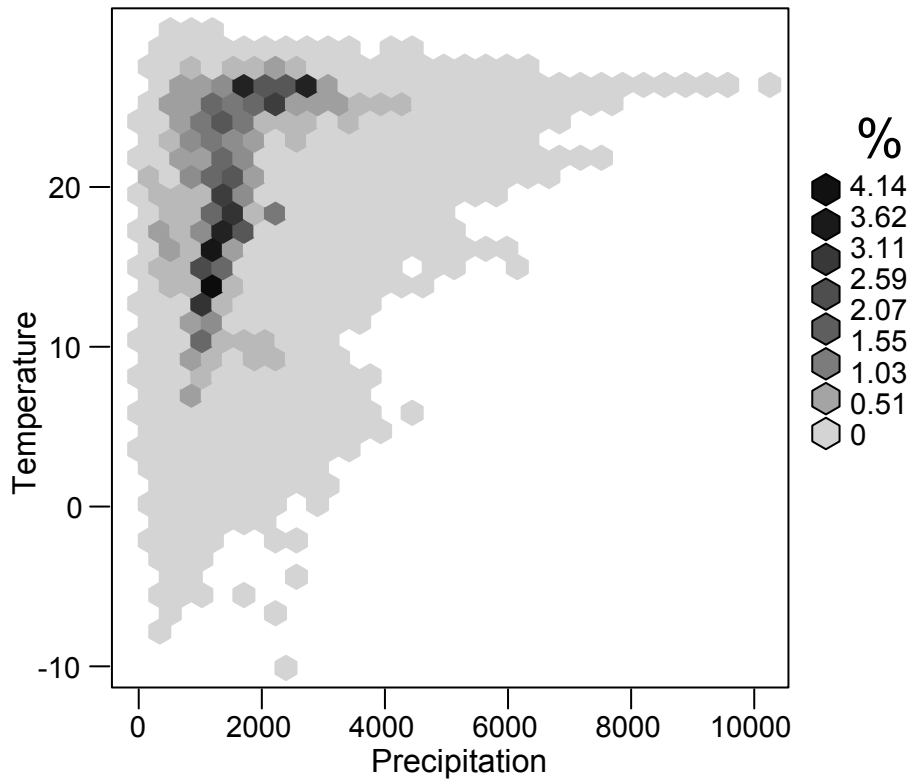
1496 **Figure S2.** Modern Ecosystem Map of the Cocinetas basin. Independent variables used to  
 1497 predict ecosystem class within a random forest classification: (a) elevation, (b) slope,  
 1498 distance to coastline, (d) distance to streams, (e) geologic units, (f) land cover, (g) red-band  
 1499 reflectance, (h) shortwave-infrared-band reflectance, (i) Normalized difference vegetation  
 1500 index NDVI.  
 1501



1502

1503 **Figure S3.** Map of the Guajira Peninsula with the geographic location of meteorological  
 1504 stations. Stations in blue record monthly precipitation with average annual precipitation in  
 1505 parenthesis. Stations in red record monthly temperature. Map color scale represents terrain  
 1506 elevation in meters above sea level (masl).

1507



1508

1509

**Figure S4.** Training dataset for the climatic model. We used 1,142,524 occurrences but the environmental distribution is unequal with fewer datapoints in the dry end of the precipitation spectrum that could produce a bias in the climatic estimation.

1510

1511

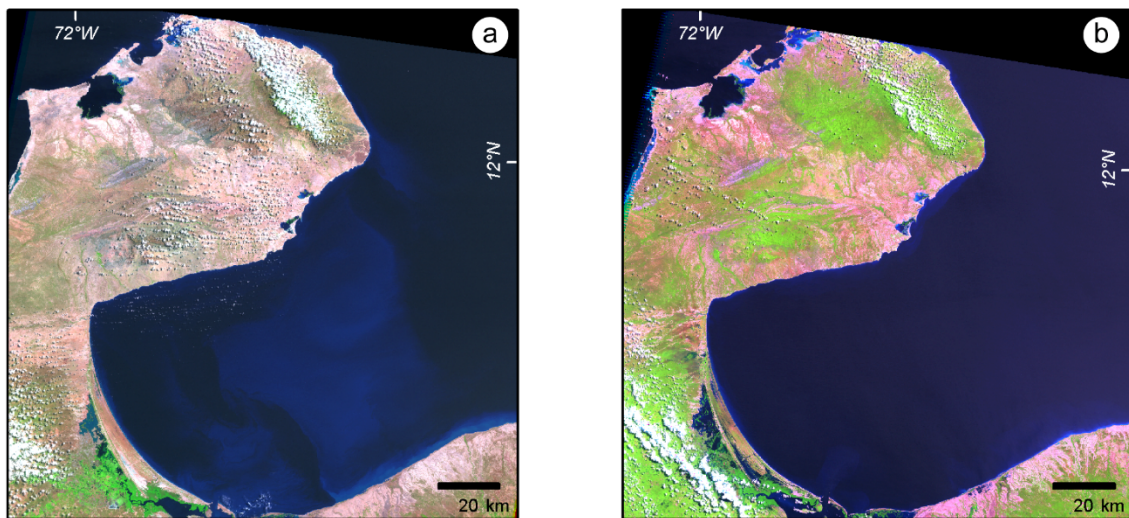
1512

1513

1514

1515

1516



1517

1518

**Figure S5.** Landsat images during (a) El Niño and (b) La Niña events. (Landsat imagery courtesy of the U.S. Geological Survey)

1519

1520

1521

1522

**Table S1.** Historical Accounts of vegetation in the Guajira Peninsula.

Ecosystem	Term	Cabo de la Vela 2, 3, 5, 7, 11, 12	Coro <sup>, 3,</sup> 4, 6, 10, 11, 12	Maracaibo 3, 7, 11, 12	Sinamaica 7, 12	Riohacha 1, 3, 6, 8
Xerophytic	Barren Land	2	2	1	1	0
Xerophytic	Cardos	3	3	1	0	0
Xerophytic, Savanna, Woodland	Farming	1	3	0	0	0
Xerophytic, Savanna, Woodland	Fauna	2	7	4	1	1
Savanna, Woodland	Fertile Land	1	3	0	2	1
Xerophytic, Savanna, Woodland	Fruit	0	2	2	1	2
Xerophytic, Savanna	Herbs and roots	0	0	3	0	1
Xerophytic	No food	1	1	0	0	0
Xerophytic	No water	1	2	1	0	1
Savanna	Lagoon	0	0	1	2	0
Xerophytic, Savanna	River	0	2	4	4	3
Xerophytic	Sand	1	0	0	0	1
Xerophytic	Savanna	5	4	3	5	1
Woodland	Sierra	4	3	6	5	1
Xerophytic, Savanna	Small Trees	0	2	0	0	0
Savanna	Swamp	0	0	0	4	0
Xerophytic	Thorns	2	1	1	0	0
Xerophytic, Savanna	Trees	1	4	0	1	1
Xerophytic, Savanna	Valley	1	0	4	3	0
Xerophytic, Savanna	Water Birth	0	0	0	0	0

1. (Ballesteros, 1962); 2. (Bolivar, 1972); 3. (Castellanos, 1847); 4.(Federman, 1958); 5.

(Fernández de Oviedo y Valdés &amp; Pérez de Tudela y Bueso, 1959); 6. (López de Velasco, 1964);

7. (Martin, 1962); 8. (Navarrete &amp; Barbudo, 1964); 9. (Naveros, 1962); 10. (Ocampo &amp; Montalvo

de Jarama, 1956); 11. (Oviedo, 1986);12. (Tolosa, 1964)

1529 **Table S2.** Data sources for modern ecosystems map.

1530

Data	Source	Relevant characteristics
Training points	Field data, Geoeye-1 imagery, Google Earth	Geoeye-1 image from 2009-07-13, spatial resolution: 2 m and 0.5 m (multispectral / panchromatic)
Elevation	IGAC <sup>1</sup>	1:25,000 scale
Slope	From elevation data	
Distance to coastline	Coastline from Spot-5 imagery	
Distance to streams	Streams from IGAC <sup>1</sup>	
Geologic units	(Moreno et al., 2015)	
Soil mapping units	(MADS, 2015)	1:100,000 scale
Land cover	(MADS, 2015)	1:100,000 scale
Reflectance & Normalized difference vegetation index (NDVI)	Spot-5 imagery	Image date: 2007-02-10 Spatial resolution: 10m

1531 1 Colombia's National Geographic Institute

1532

1533 **Table S3.** Location of Holocene samples

1534

Sample Label	Locality ID	Lat	Long
37069_S2	720001	11.23	-70.25
Aytiamanox Point	220073	11.92	-71.31
Aytiamanox Point 2.1m	220073	11.92	-71.31
Aytiamanox Point 2m	220073	11.92	-71.31
CJ-Jimolletes	220073	11.92	-71.31
FM240114-10	220039	11.90	-71.32
FM240114-6	220039	11.90	-71.32
JHE-0011	220039	11.90	-71.32
FM240114-5	220039	11.90	-71.32
Tukakas Jheoo_Muestra sed. Agua	220039	11.90	-71.32

1535

1536

1537